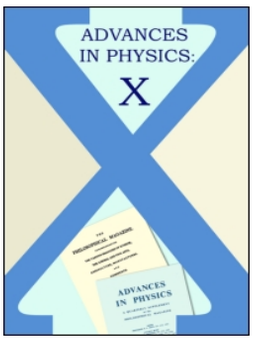

Advances in Physics: X

ISSN: (Print) 2374-6149 (Online) Journal homepage: http://www.tandfonline.com/loi/tapx20

Recent progress on liquid metals and their applications

Guyue Bo, Long Ren, Xun Xu, Yi Du & Shixue Dou

To cite this article: Guyue Bo, Long Ren, Xun Xu, Yi Du & Shixue Dou (2018) Recent progress on liquid metals and their applications, Advances in Physics: X, 3:1, 1446359, DOI: 10.1080/23746149.2018.1446359

To link to this article: https://doi.org/10.1080/23746149.2018.1446359

Published online: 05 Mar 2018.

ADVANCES IN PHYSICS: X, 2018
VOL. 3, NO. 1, 1446359
https://doi.org/10.1080/23746149.2018.1446359

Taylor & Francis
Taylor & Francis Group

REVIEW ARTICLE

OPEN ACCESS Check for updates

Recent progress on liquid metals and their applications

Guyue Bo[#], Long Ren[#], Xun Xu, Yi Du and Shixue Dou

Institute for Superconducting and Electronic Materials (ISEM), Australian Institute for Innovative Materials (AIIM), University of Wollongong, Wollongong, Australia

ABSTRACT

Gallium-based liquid metals show excellent thermal and electrical conductivities with low viscosity and non-toxicity. Their melting points are either lower than or close to room temperature, which endows them with additional advantages in comparison to the solid metals; for example, they are flexible, stretchable and reformable at room temperature. Recently, great improvements have been achieved in developing multifunctional devices by using Ga-based liquid metals, including actuators, flexible circuits, bio-devices and self-healing superconductors. Here, we review recent research progress on Gallium-based liquid metals, especially on the applications aspects. These applications are mainly based on the unique properties of liquid metals, including low melting point, flexible and stretchable mechanical properties, excellent electrical and thermal conductivities and biocompatibility.

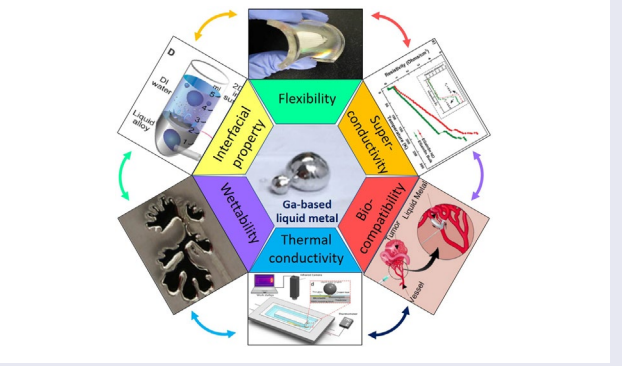

ARTICLE HISTORY
Received 31 October 2017
Accepted 23 February 2018

KEYWORDS
Liquid metal; gallium; room temperature; eutectic; applications

PACS
61.25.Mv, % Liquid metals and alloys; 72.15.Cz, % Electrical and thermal conduction in amorphous and liquid metals and alloys; 68.03.Cd, % Surface tension and related phenomena; 74.25.-q, % Properties of superconductors

Introduction

Metals are the most important and earth-abundant materials. Ninety-one of overall one hundred eighteen elements are metals. They generally exhibit good

CONTACT Yi Du yi_du@uow.edu.au
[#]Authors who contribute equally to this work.

electrical and thermal conductivity, excellent mechanical properties and unique chemical properties, which can be widely used in applications ranging from conductive wires, thermal conductors, structural frames and pipes, to coatings, medicines and catalysts. Most of the metals are in the solid state at room temperature. Exceptions include francium (Fr), caesium (Cs), rubidium (Rb), mercury (Hg) and gallium (Ga), which can be defined as *liquid metals*. Their melting points are either lower than or close to room temperature, which enable them to remain in the liquid state at room temperature [1]. This brings them additional advantages in comparison with the other metals; for example, they are fluid, stretchable and reformable at room temperature [2]. Unfortunately, the intrinsic radioactivity of Cs, extreme instability of Fr and Rb and toxicity of Hg limit their applications to certain specific areas [1]. Ga, on the other hand, is a metalloid element, but it still shows metallic properties when it is in solid phase and becomes a superconductor at extremely low temperature [critical temperature $T_c \approx -272.06$ °C (1.09 K)] [3]. Its high boiling point allows it to remain in the liquid phase from near room temperature to approximately 2403 °C [4]. It demonstrates great potential for common uses as a liquid metal to realise flexible, stretchable and self-healing electrical devices [2], although its melting point (29.7 °C) is still slightly higher than room temperature [4].

Recently, it was found that the Ga-based eutectic alloys, such Ga–Indium (EGaIn), Ga–Tin (EGaSn) and Ga–In–Sn (EGaInSn, Galinstan) systems show tunable melting temperatures from −19 °C to far above room temperature, depending upon their component ratio [5,6]. In addition, these alloys show typical metallic properties in contrast to the metalloid nature of Ga, even in the liquid phase. Owing to these unique properties, research on Ga-based liquid metals has attracted great attention and made several significant breakthroughs very recently. Here, we will review current progress on the exploration and development of Ga-based liquid metals and their properties. The novel applications based on these properties will be discussed.

Ga-based liquid metals

Ga was discovered in 1875. It is a relatively ideal liquid material to replace mercury due to its low vapour pressure [2], low toxicity, low viscosity [7] and metallic electrical conductivity performance [2]. Its melting point, however, 29.7 °C [4], is slightly higher than room temperature [8]. In order to decrease its meting point, eutectic Ga alloys have been developed. Indium was the first element that was alloyed with Ga. The melting point of EGaIn can be tuned to as low as 15 °C when it is incorporated at 14 wt%, as shown in Figure 1 [5]. Later, Sn was introduced into EGaIn (Figure 2), and the alloy was denoted as EGaInSn. Its melting point can be decreased to −19 °C. Various liquid phases were identified and are summarised in the phase diagram, as shown in Figure 2 [6]. The tunable melting temperatures of EGaIn and EGaInSn represent one of the most significant steps toward

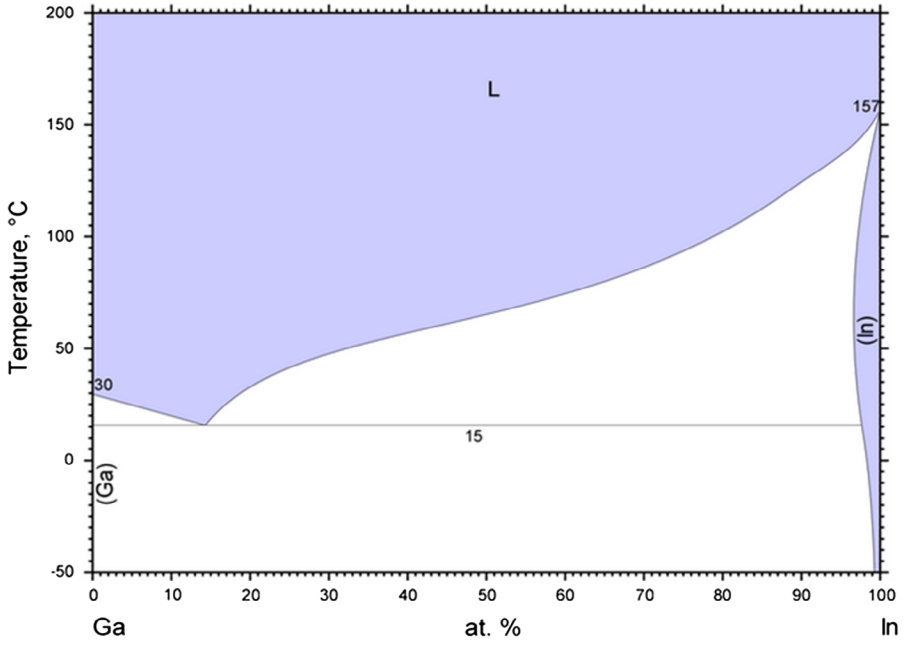

Figure 1. Phase diagram of eutectic gallium–indium [5].

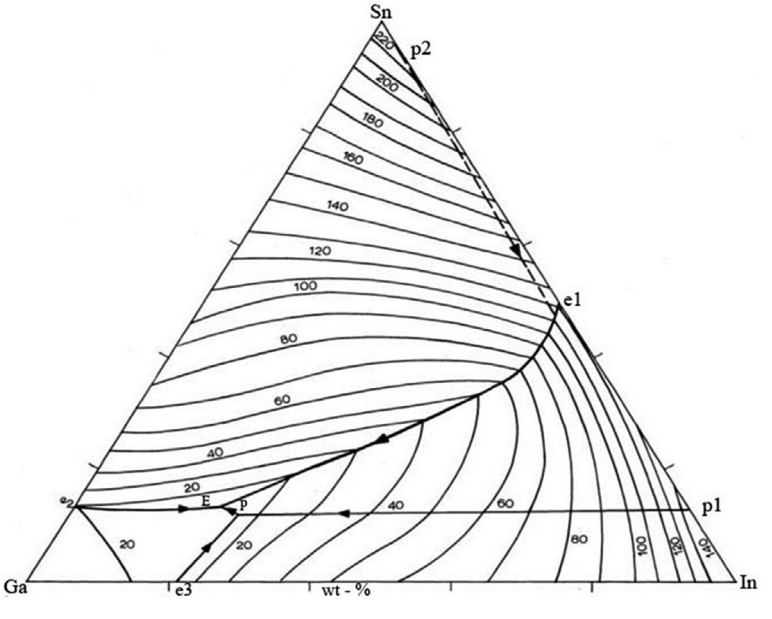

Figure 2. Eutectic gallium–indium–tin phase diagram [6].

application of Ga-based alloys as liquid metals. Note that corrosive property of Ga towards almost all the metals [9] (except Tungsten (W) and Tantalum (Ta)) has to be considered before using EGaIn and EGaInSn in devices. Most of the

liquid-metal-based flexible and stretchable devices have had to be sealed properly in polymer frames or channels [10]. Chemical passivation is an intrinsic property of Ga that enables Ga and Ga-based alloys to be used as dielectrics, although it also hinders their general use as liquid conductors. The surfaces of pure Ga or eutectic Ga-based alloys are easily oxidised and form an amorphous Ga oxide layer in the ambient environment that decreases the surface tension of the liquid metal [11–13]. The thickness of the intrinsically formed Ga oxide surface layer is 0.5–3 nm [14–16]. Nevertheless, the thickness of the oxide layer can be modulated by using an electrochemical method. Consequently, the dielectric functions of Ga and the eutectic Ga alloys can be tuned from 1.24 to 3.1 eV at room temperature. For the purpose of electric applications, the surface oxide layer can be eliminated by applying an electrochemically reductive potential or simply removed by diluted acids/strong alkaline media [17].

Properties and applications of gallium-based liquid metal

The good electrical and thermal properties and the unique mechanical, fluidic and surface properties of Ga-based liquid metal offer great potential for applications in functional electronics, flexible devices, actuators and bio-devices. There are now several excellent reviews covering applications of liquid metal on different specific properties [1,8,11,15,16]. Here, we will cover the current progress on the main advantaged properties of Ga-based liquid metal and the applications derived from these advantages.

Electrical properties and applications

The resistance of Ga is higher than that of copper, but the conductivity of Ga-based liquid metal is much higher than for other liquids. The conductivity of Ga in the solid state is poorer than in the liquid state [18]. C. Dodd have measured the resistivity of Ga (Figure 3), the variation of resistivity with temperature is linear [19].

High electrical conductivity electronics at room temperature

With the benefit of their excellent electric conductivity, Ga-based liquid metals combine the performance of metallic with fluidic properties [20]. They can be injected into micro-channels at room temperature to make flexible electronic components, such as antennas. Dickey et al. reported a procedure to fabricate reversibly tunable fluidic antennas (Figure 4) [21]. They utilised photolithography to make a pattern for the dipole on (polydimethylsiloxane) (PDMS) layer on a silicon slide. After exposure of this substrate to oxygen, the substrate was sealed to generate micro-channel, and then liquid metal was injected into the microfluidic channels to form the antenna. The resonance of antenna is approximately 1962 MHz, and the radiation efficiency is 90% in far field measurements. (Efficiency of 100% means that the antenna has no losses.) Thus, the electrical loss of EGaIn antennas

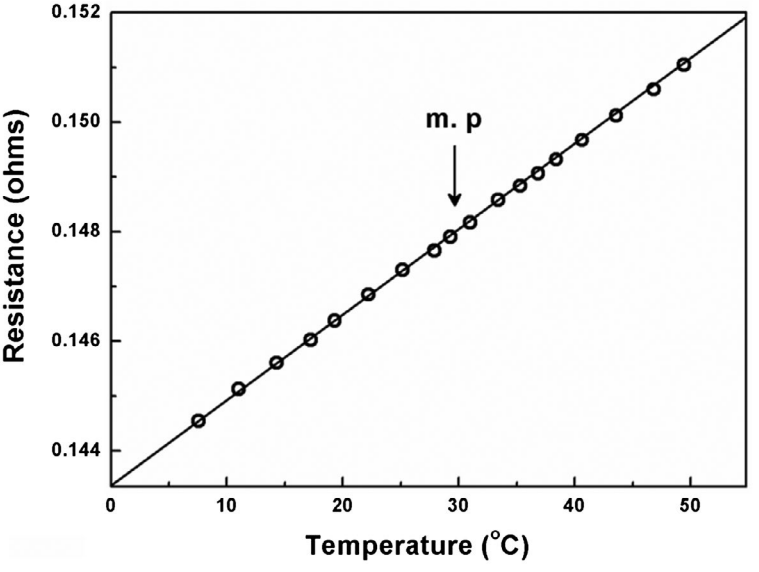

Figure 3. Temperature coefficient of resistance of Ga, reproduced from [19].

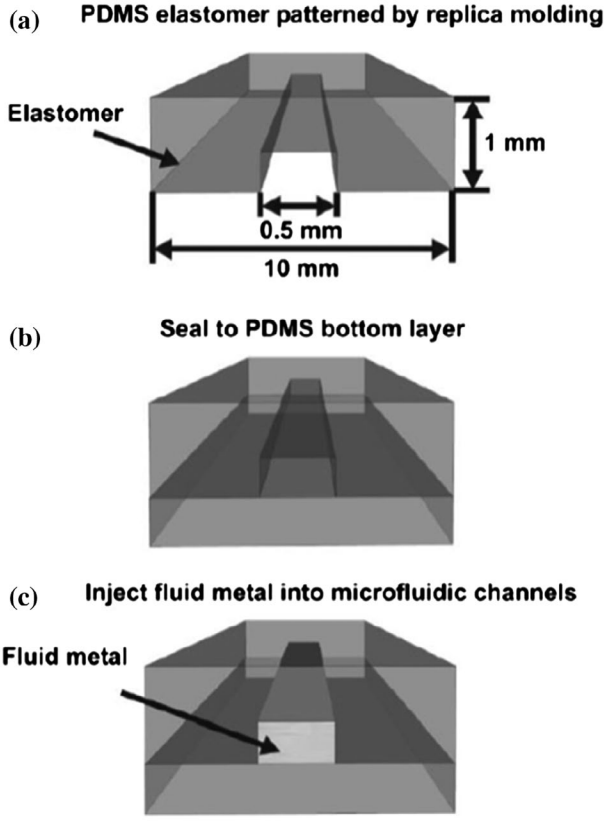

Figure 4. The process of dipole antenna fabrication. (a) PDMS elastomer patterned on substrate. (b) The PDMS channels are sealed. (c) Liquid metal is injected into the microchannels to make a dipole antenna [21].

is acceptable in applications. The novel antennas provide a simple way to fabricate components, including electronic fabric [21].

Superconductive electronics at low temperature

A superconductor is a type of material that shows zero electrical resistance and the Meissner effect, when the temperature is below a certain critical temperature (T_c). Conventional superconductors have some drawbacks, for example, they are fragile and subject to processing difficulties. The superconducting transition temperature of pure Ga is lower than −268.95 °C (4.2 K) [3], the boiling temperature of helium. This is a barrier to practical applications of this material as a superconductor. Ren et al. found that the superconducting transition temperature for GaInSn alloy can be tuned by the component ratio [22]. The highest T_c in this family is −266.55 °C (6.6 K), which is higher than liquid helium temperature. It was found that liquid metal nanoparticles also retained the same superconductive properties as their bulk material. (Figure 5) [22]. These nanoparticles were dispersed into aqueous solution with organic dispersants (surfactants). A superconducting ink can be then developed by using such the dispersive nanoparticles, which can be directly used for inkjet printing. The micro-/nano-circuits have been printed by such inks, which displays mechanical flexibility and superconducting properties. This work indicates that liquid metal superconductor may be used for microscale nuclear magnetic resonance (NMR), micro-/nano-superconducting coils, flexible superconducting electronic components and other applications [22].

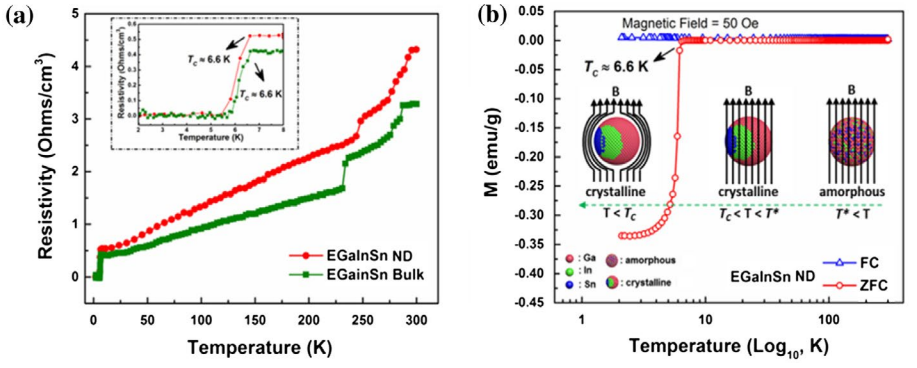

Figure 5. (a) Superconducting transition temperature for EGaInSn bulk materials and nanoparticles, with the inset showing an enlargement of the transition. (b) Temperature dependence of the magnetisation of EGaInSn nanodroplets; the inset schematic illustrations show that the EGaInSn nanodroplet would make the transition to crystalline from amorphous as the temperature decreases from room temperature (300 K) to T* (133 K, the fully crystalline temperature point of EGaInSn nanodroplets (NDs)). The amorphous and then the crystalline EGaInSn nanodroplet remains paramagnetic when the temperature is above the T_c (≈6.6 K), but the crystalline EGaInSn nanodroplet will change to diamagnetic when the temperature falls below T_c (≈6.6 K) due to the Meissner effect [22].

Thermal properties and applications

Similar to most metallic materials, Ga and its alloys also show high thermal conductivity [13]. The thermal conductivity of pure Ga is 28.7 kcal/m•h•°C, which is much higher than the thermal conductivity of air or water [23]. Furthermore, the liquidity and high thermal conductivity of Ga-based liquid metals allows them to be used as coolant agents for several applications, such as microdevices [24].

Coolant

Heat dissipation management is important for cooling the compact electronic packages including central processing unit (CPU) in computers [23]. The evolution of micro/nano-devices has significantly enhanced the capability of liquid cooling systems. Traditionally, water and aqueous solutions are utilised as coolant, but their low thermal conductivity reduces the effectiveness of heat dissipation. As an alternative, Ga-based liquid metal coolants were developed in recent years, owing

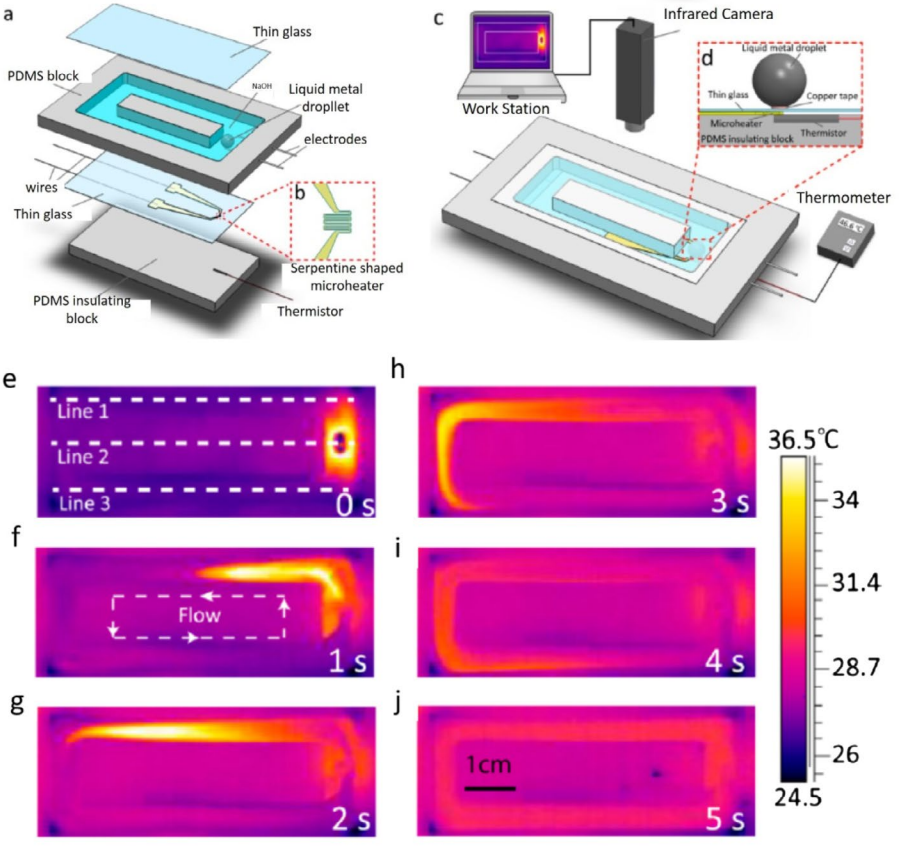

Figure 6. (a–d) Schematics for liquid metal cooling experiment system. (a) Exploded image. (b) Image of Serpentine shaped microheater. (c) Schematic of cooling system assembling. (b) Close-up image of EGaInSn marble is placed onto the hot spot. (e–j) Sequential snapshots display the alterations of temperature with respect to time [26].

to their intrinsic liquidity and high thermal conductivity [25]. Khoshmanesh et al. designed an integrated liquid cooling system by utilising a small droplet of liquid metal Galinstan (commercial GaInSn alloy) [26]. Figure 6(a)–(c) schematically displays an image of this liquid metal-based cooling system. The device facilitates the effective delivery of heat from resistive heater into the stream of liquid by the circulated and high thermal conductive liquid metal droplet in the cooling solution. Sequential snapshots presented in Figure 6(d)–(i) show the variations of temperature of the cooling channel with respect to time. The graphs clearly show the non-uniform distribution of temperature along the cooling channel, before actuating the liquid metal droplet (t = 0 s). Upon application of a square wave dc signal, the liquid meal droplet serves as a pump, driving the coolant medium through the cooling channel [26].

Mechanical and fluidic properties and applications

Ga and its alloys show passivation behaviour with the formation of a surface oxide layer when exposed in air. The oxide skin (0.5–3 nm thick) arising from intrinsic passivation further promotes the chemical and mechanical stability of the liquid metals [27,28], and in particular, it leads to non-Newtonian fluidic performance [2]. The mechanical properties cannot be changed because the Ga-based liquid metals are in the liquid phase around room temperature [16].

Flexible and stretchable electronics

Flexible and stretchable electronics have components and circuits that can retain their function while being deformed. Conventional flexible electronics are made of rigid materials, for example aluminium (Al) and copper (Cu). They could be rendered flexible by making them sufficiently thin [8]. The flexibility of these classical solid antennas electronics is not adequate, however, since they could be still damaged by metal fatigue and the conductivity of the electronic systems might be influenced. Due to its liquid form at room temperature, Hg has been considered for application in flexible electronics, but its toxicity is a huge barrier to this. The large surface tension of Hg is too high, which may not allow spontaneous recovery deformation. In contrast, Ga and its alloys avoid the toxicity problem, and the oxide skin provides mechanical stability to Ga-based liquid metal [29], which is significant for conformal and flexible electronics. Owning to the intrinsic liquid property at room temperature, Ga-based liquid metal can be reshaped easily while remains metallic function. Thus, it can be injected into stretchable channels [30]. Hayes et al. developed a flexible multi-layer antenna, which was constructed by liquid metal (EGaIn) injecting into the microstrip. This antenna can be flexed without any great change in function (Figure 7(a) and (b)) [31]. It could be also used to make a conductor with excellent mechanical performance [8]. As shown in Figure 7(c) and (d), Zhu et al. fabricated a stretchable liquid metal conductive fibre which could be stretched to 600% without any loss of conductivity, and

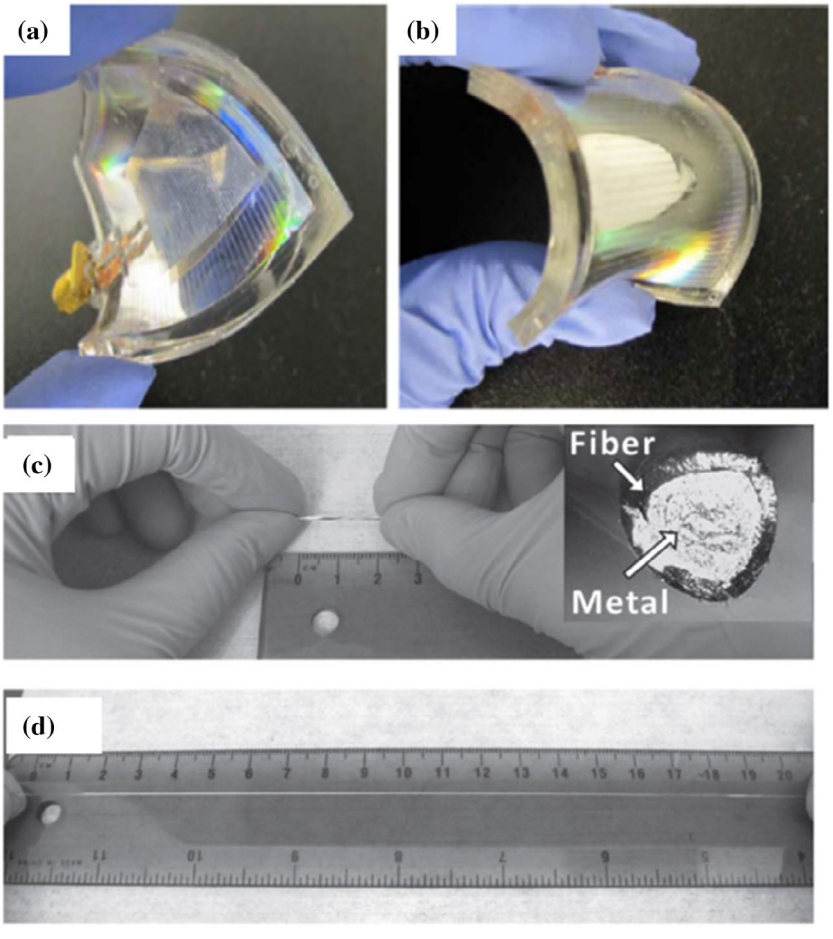

Figure 7. Images of a liquid metal-based flexible and stretchable electronic device. (a–b) Flexible microstrip patch antenna made from liquid metal [31]. (c–d) An EGaIn wire can be stretched by 800% [30].

800% could be achieved before breaking [30]. Even though the conductivities of Ga and its alloys are lower than for Cu, these materials are acceptable due to their additional advantages, including stretchability, flexibility and deformation [8]. Ga-based liquid metals have also demonstrated the potential to be utilised in diffraction gratings [32], metamaterials [33], etc.

Self-healing devices

Self-healing wires can improve the durability of many electronic devices, especially for stretchable electronics [34–37]. In addition to that, self-healing wires create a novel approach to the rewiring of circuits, as they offer a simple way to reconfigure micro-channels, which be set in complex shapes and systems. Traditionally, conductive polymers have been used as self-healing conductive materials [38–41], although those materials could only self-heal at high-temperature (~200 °C). The

conductivity of the polymers is much worse than for metals [42]. Ga-based Liquid metals can solve these problems. Li et al. created a light emitting diode (LED) integrated EGaInSn circuit. In this self-healing device, the liquid metal wire can be cut by shears, and then heals by itself under ambient conditions without an additional force to reconnect the broken wire. [43] Palleau et al. also fabricated self-healing stretchable circuits by using Ga-based liquid metal [10]. The wires are fabricated in self-healing polymer micro-channels, which are injected with liquid metal (EGaIn). The circuits can self-heal, not only mechanically, but also electrically after being cut. Figure 8(d)–(f) shows the self-healing procedure for the stretchable wire in the above work. Initially, a LED, a wire and a voltage power supply form a circuit (Figure 8(d)), it was cut into two pieces (Figure 8(e)), then the oxide skin forms rapidly. The oxide skin precludes the liquid metal from returning into the microfluidic channels. Moreover, the oxide layer helps EGaIn adhere to polymer. This stretchable property may be useful in the field of stretchable electronic and reconfigurable circuit fabrication [10].

Reconfigurable filter and antenna

Traditional microstrip filters are made using printed circuit board technology [44,45], which methods often used is etching the pattern on stacked copper sheets [38]. Alteration of the electrical length of the stub and response of the filter, however, require a number of steps and approaches, for instance, using the incorporation of varactors to bridge the disconnected part of the stub [39]. In contrast, Khan et al. demonstrated a simple way to fabricate tunable filters, which combines an insulated soft polymer and conductive liquid metal that can respond to an electrical signal when there is sufficient pressure (Figure 9(a)) [38]. Based

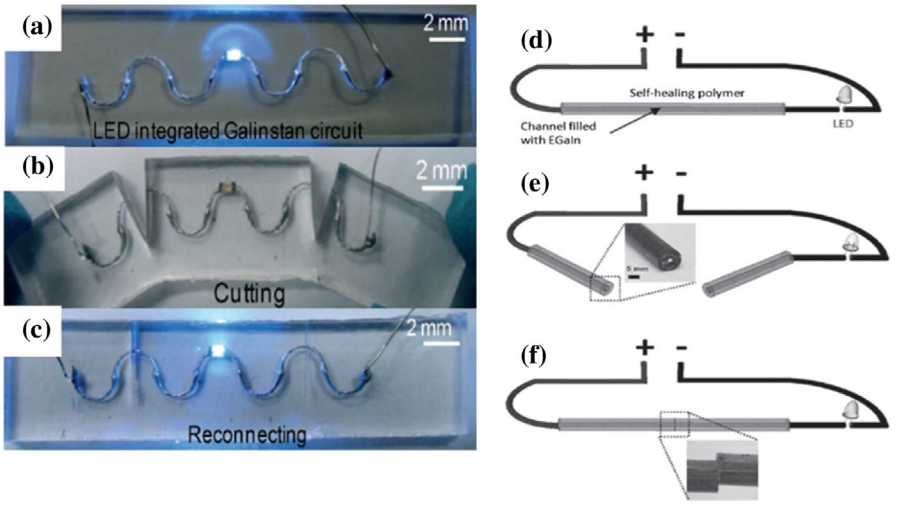

Figure 8. (a–c) Images show the self-healing of a galinstan circuit integrated with a LED [43]. (d–f) Schematic diagrams showing the disconnection and reconnection of a simple electronic circuit using a self-healing wire [10].

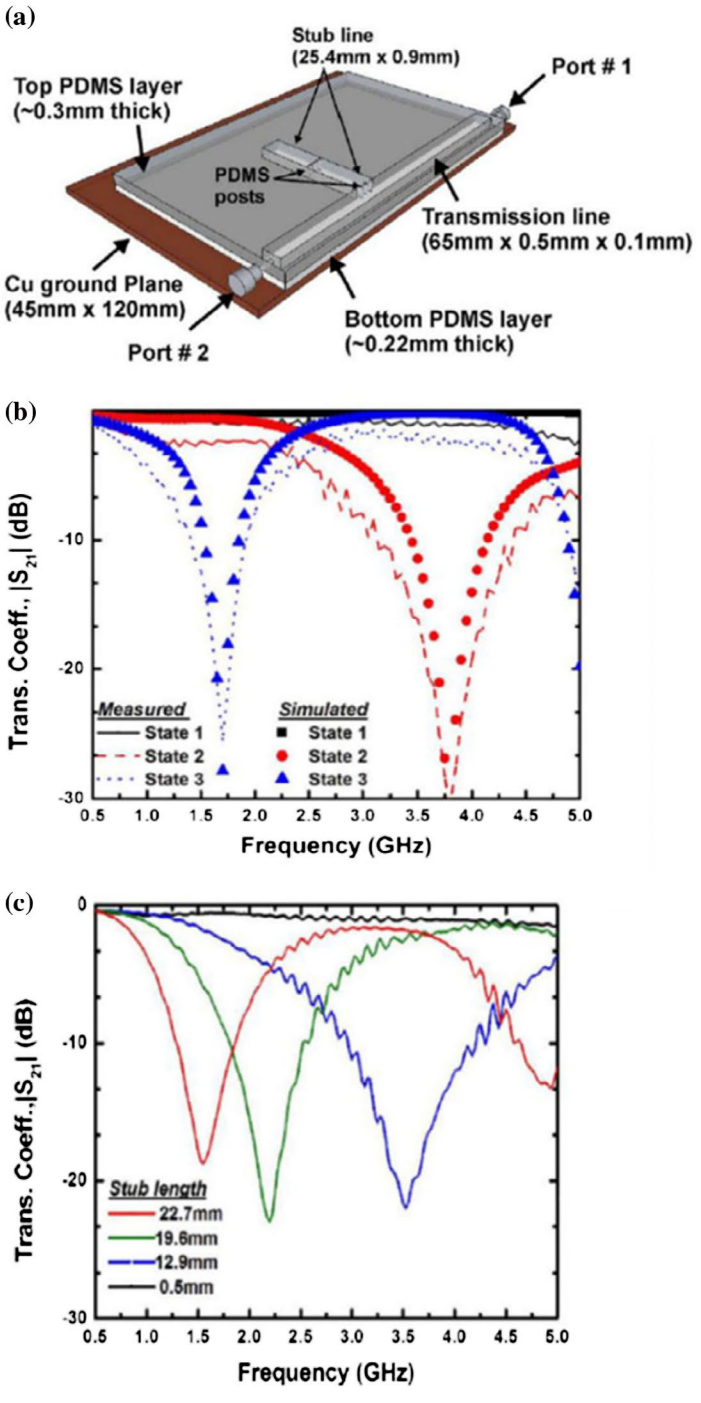

Figure 9. Image of bandstop filter. (a) Geometry of bandstop filter with a 50 Ω microstrip transmission line from Port 1 to Port 2 and an open stub section. (b) Measured and simulated transmission coefficient response for each state of the microstrip filter. The frequency of the filter becomes lower with increasing stub length. (c) Measured transmission coefficient of a prototype with an open stub shortened from 22.7 to 0.5 mm [38].

on typical transmission coefficient measurements and simulations relative to the resonant frequency, Figure 9(b) illustrates that the resonant frequency would decrease with increasing stub length (relative to the pressure). More importantly, the mechanical stability arising from the oxide skin of the liquid metal gives this bandstop filter the ability to operate reversibly. This technology can also be applied in wearable devices [38].

A reconfigurable antenna is also a specific type of electronics, which supports dynamic control of its frequency and shape [40]. Most conventional antennas fail to enable reconfiguration without any additional components [41,46,47]. Khan et al. designed a novel frequency shifting antenna fabricated from liquid metal alloys (Figure 10) [48]. In details, the innermost two segments and outermost

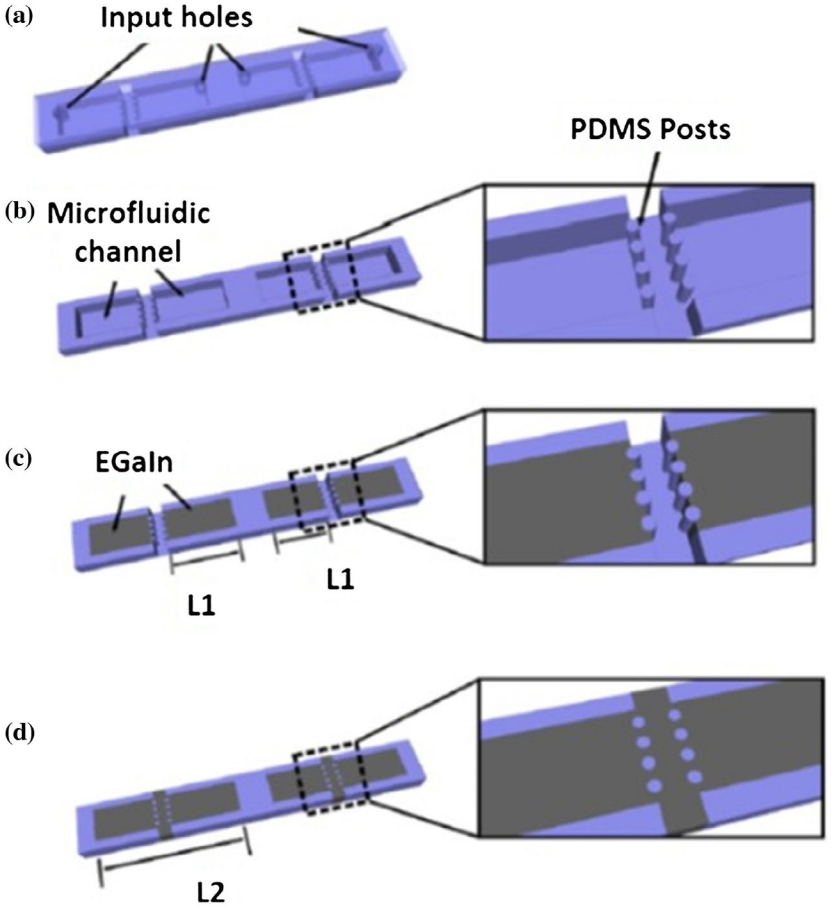

Figure 10. Schematic illustration of reconfigurable antenna. The shape reconfigurable antenna can be changed by pressure. (a) The empty microfluidic channels with inlet holes. (b) The antenna is separated by rows of posts. (c) Liquid metal has been injected into the microchannels. Initially, the metal does not flow until the pressure exceeds the critical pressure. (d) The four sections of metal merge into two longer sections (each of length L2), which lowers the resonant frequency [48].

two segments are separated by two post rows. Then, the EGaIn liquid metal is injected into inlet holes, and it fills into channels easily. When the pressure exceeds a critical value, the innermost and outermost segments are merged by the flowing liquid conductive material. The shape, electrical length and frequency could be all changed and controlled by the flowing liquid metal. The liquid metal-based antenna successfully responds to an external stimulus without external switches [48].

Surface tension and wettability

The oxide skin of Ga allows Ga-based liquid metal to wet other surfaces. The oxide layer shows elastic layer which can support the maximum surface stress of 0.5 – 0.6 $N \bullet m^{-1}$. When it is broken, it reforms instantaneously and rapidly under oxygenated conditions [16]. Moreover, the surface tension of Ga is large than 400 $mN \bullet m^{-1}$ [13], the oxide layer not only lower the surface tension of Ga-based liquid metal, but also helps to remain the shape of Ga-based liquid metal and keep stable after injection [49]. As the surface or interface tension and wettability can be changed or controlled by electric-induced effect (including electrocapillarity, continuous electrowetting (CEW) and electrowetting on dielectric (EWOD)), the Ga-based liquid metal has been manipulated by applied the external electric field in different liquid-related system. Besides, the surface tension of Ga-based liquid metal can be also affected by modification of the liquid electrolyte surrounding it, which has been demonstrated as an effective way to actuate liquid metal droplets. Regardless of the applied different external fields, the liquid metal driving mechanism could be attributed to the changes of electrical double layer forming on the liquid droplet surface. Placing Ga-based liquid metal in the electrolyte, according to the Stern's electrical double layer (EDL) theory, two ion layers with opposite charges and equal electrical quantity would exist in the interface between the electrolyte and liquid metal to form an EDL as interface capacitor that stores electric energy. When applying a driving force, such as electrical field, magnetic field and the electrolyte ionic imbalance, the charge symmetry that exists on the surface of a liquid metal would be broken. It causes the surface tension gradient of the liquid metal droplet in electrolyte medium and generates a differential pressure. As a result, the liquid metal moves or deforms [50–52].

Actuator and pump

Actuator and Pump is a type of devices that transfer non-mechanical external energy to mechanical energy [53,54]. Gough et al. studied about the electrocapillary actuation of EGaInSn marble [54]. The external voltage was applied across the EGaInSn–electrolyte surface directly to create interfacial tension gradient making the pressure between electrolyte and droplets imbalance. This approach can be utilised to control the liquid metal flow in complex channels. However, the shape of liquid metal cannot be controlled stably due to the surface tension is

very high. In recent years, Hu et al. reported a method to solve this problem [55]. They developed a system placing liquid metal marble in an alkaline electrolyte, the droplet on the graphite surface can transformed to a flat and dull puddle with applied voltage in the electrolyte. Therefore, the liquid metal puddle can be controlled into various stable shapes due to the interactions between graphite and liquid metal. Figure 11 (a) and (b) displays a scheme for the experiment [55]. It demonstrates that the liquid metal droplet elongated and moved toward cathode with the tail-like rear when both of the cathode and anode are fixed, and external electric field be applied. This approach provides a novel method for soft device manufacture and offers a way to explore electrochemical performance of liquid metal [55]. In addition to using conductive electrolyte, Holcomb et al. introduce a technique to actuate liquid metal that uses acidification of nonconductive siloxanes to remove and prevent oxidation of liquid metal [56]. The siloxane oil

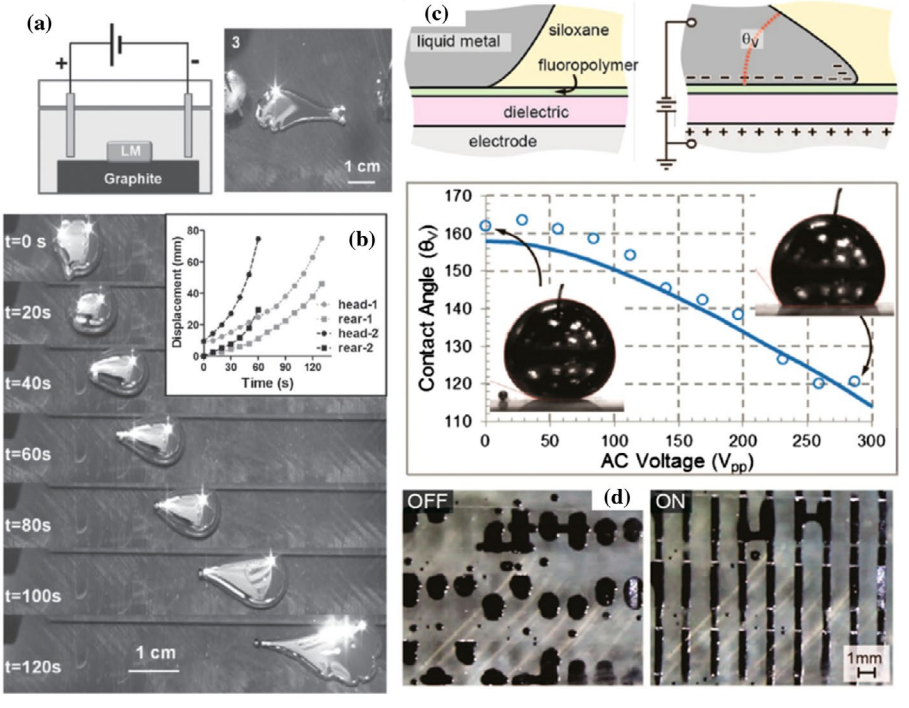

Figure 11. (a) The transformation of liquid metal marble on graphite connecting an external voltage directly with an electrode. Both of the cathode and anode are fixed and installed relatively far away from liquid metal, the marble stretched and moved toward cathode, the shape of liquid metal likes a tail. (b) The sequential snapshot for the directional locomotion of liquid metal in NaOH. The inset shows the transient displacements of head and rear of two sized liquid metal droplets. (The diameter of liquid metal droplet 1 is 8.5 mm and droplet 2 is 9.6 mm) [55]. (c) Schematic displays illustration of the procedure of for electrowetting on dielectric. It is with a graph showing the relationship of between the contact angle and the applied electrical potential. (d) Images of a switchable wire-grid polarizer device. The liquid metal is in the form of droplets when no electric potential is applied. When the bias is applied, the liquid metal changes to line shapes [56].

combines hydrochloric acid with hydrobromic acid, which is chemically stable and can promote better electrowetting. This approach offers new opportunities to fabricate devices for applications of liquid metal. Figure 11(c) shows the procedure for electrowetting on dielectric for gallium alloys in the HCl siloxane with about 0.135 M HCl. The liquid metal is surrounded by insulating material on an electrode which is separated by a dielectric layer. The contact angle was expected to be 180° without voltage, but it was measured to be 160° due to the influence of gravity and other factors. When bias was applied, the contact angle changed to nearly 120° at 300 V [56]. Figure 11(d) shows a switchable wire-grid polariser system, which is one application for this concept. Liquid metal is in the form of droplets with no applied voltage. When a bias is applied, the liquid metal changes to a line shape [56]. EWOD is a novel method that provides many benefits, including easy fabrication and no moving parts.

Strategies other than electrical filed have been also developed to actuate liquid metal, Zavabeti et al. showed an novel approach that only utilises the ionic imbalance of aqueous electrolyte surrounding the liquid metal [57]. The PH and ionic concentration gradients across liquid metal are significant factors for liquid metal actuation. Figure 12(a) and (b) shows the PH imbalance induced the pressure imbalance on two sides of liquid metal droplet, thus, liquid metal droplet moves from HCl (high surface tension) side to NaOH (low surface tension) side. Therefore, ionic properties for electrolytes contain enough energy to induce the liquid metal marble movement, the marble can move without electric field. The outcomes of this work can be utilised to fabricate future autonomous low dimensional micromechanical components which are based on the changes of compositional of electrolytes [57].

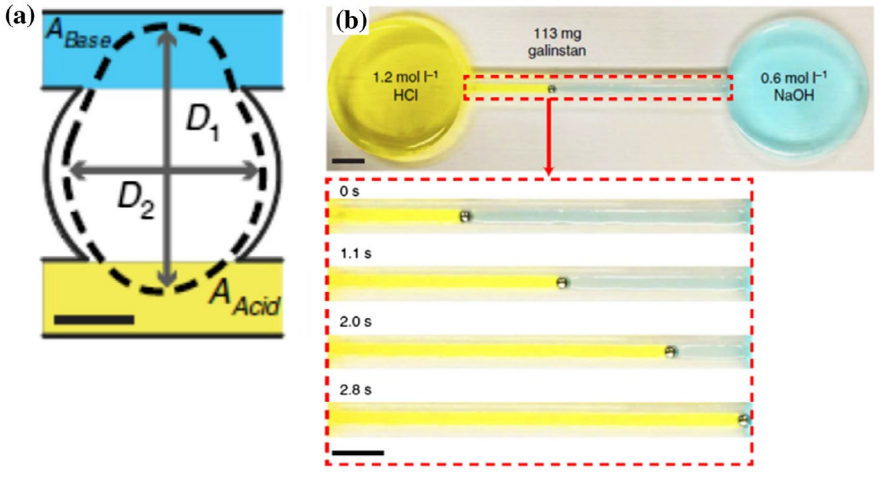

Figure 12. (a) Schematic of surface tension (b) Liquid metal droplet moves from 1.2 mol/L HCl to 0.6 mol/L NaOH [57].

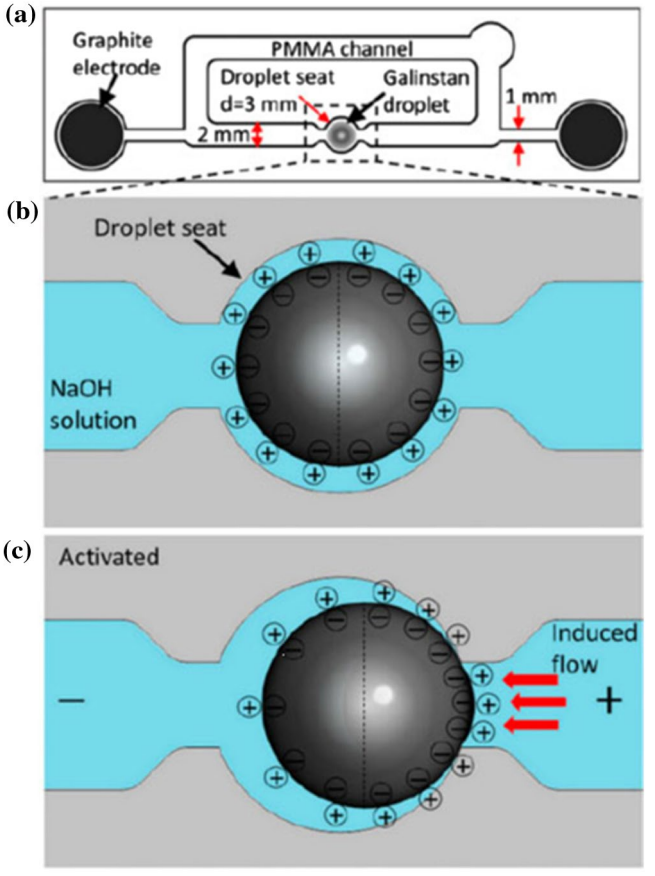

Figure 13. Principle of the liquid metal enabled pump. (a) Schematic diagram of the system. (b) Schematic illustration of the charge distribution of EGaInSn droplets without bias. (c) Schematic illustration of the charge distribution on the EGaInSn droplet when electric field is applied [58].

In addition to those simple actuation systems, Tang et al. designed a 'liquid metal enabled pump' system [58]. In this system, EGaInSn is the core of pump to transfer electrical energy to mechanical energy. Figure 13(a) shows the schematic of experiment system. The EGaInSn droplet was placed in the polymethylmethacrylate (PMMA) channel, sodium hydroxide solution was electrolyte. Figure 13(b) shows the electric double layer on the interfacial of gallium and electrolyte. Figure 13(c) displays the charge distribution of EGaInSn droplet when applied bias. Electrowetting at the surface of liquid metal droplet can enabled this pump when the dynamic electric field is applied. The pump offers various benefits, such as it can arrive to high flow rates under low power consumption, simple controlling, no moving parts and low cost [58]. Furthermore, this pump has the potential to enable applications.

Khoshmanesh et al. utilised a pair of liquid metal pumps which made by EGaInSn droplets to provide controllable vortices within a small liquid chamber. Figure 14(a) shows EGaInSn droplet was injected into channel, then the droplet deformed after activation (Figure 14(b)). Numerical simulations predict the small

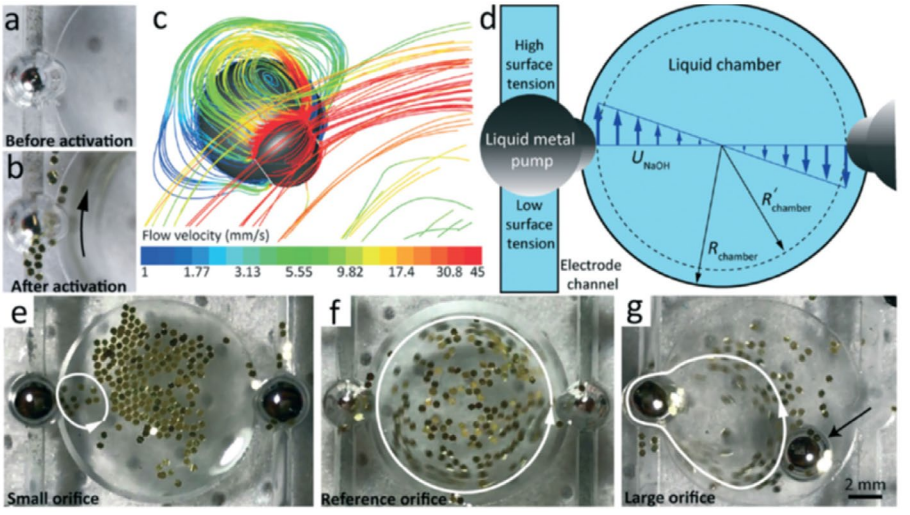

Figure 14. (a) Image showing liquid metal droplet injected into the liquid chamber before activation. (b) Image of EGaInSn droplet in liquid chamber after activation. (c)Image from numerical simulation. (d) Schematic diagram of liquid metal enabled vortex generator. (e–g) Properties of vortices in response to small, reference, and large orifices connecting the electrode channels to the liquid chamber [59].

and large vortices nearby each droplet (Figure 14(c)). The simplified theoretical model was shown in Figure 14(d). In order to understand the influence for droplet intrusion on the pumping characteristic of droplets, Khoshmanesh et al. designed a plan which use different size of orifice [59]. As a result, the small orifice causes a local vortex close to the droplets (Figure 14(e)), the reference orifice causes a large orifice embracing the whole liquid chamber (Figure 14(f)), the large orifice causes complete intrusion of one of the droplets into the liquid chamber (Figure 14(g)). They demonstrated the utility of liquid metal pumps to create customised spatiotemporal temperature profiles into a liquid chamber [59]. They use liquid metal enabled pumps inducing vortices inside a liquid chamber. This method is an excellent way to generate spatial temperature gradients by altering the rotational velocity and configuration of vortices, which can be controlled by changing the frequency and polarity. This approach replaced the method of using acousto thermal [11,57] or microwave-induced heating, it means that the system does not require a lot of hot spots [13] or localised hot spots for heating in the liquid. These pumps can generate more complex temperature profiles and gradients [59].

Transformation

As Ga-based liquid metals have mechanical stability, they can be transformed into different shapes around room temperature by utilising various applied forces [20,60,61]. Khan et al. introduced the oxide layer of liquid metal can be formed and withdrawn by low voltages [62]. Figure 15 displays the electrocapillarity-induced liquid metal removal from micro channels. It demonstrates that the oxide skin is an excellent surfactant for metals, and liquid metal can be removed and

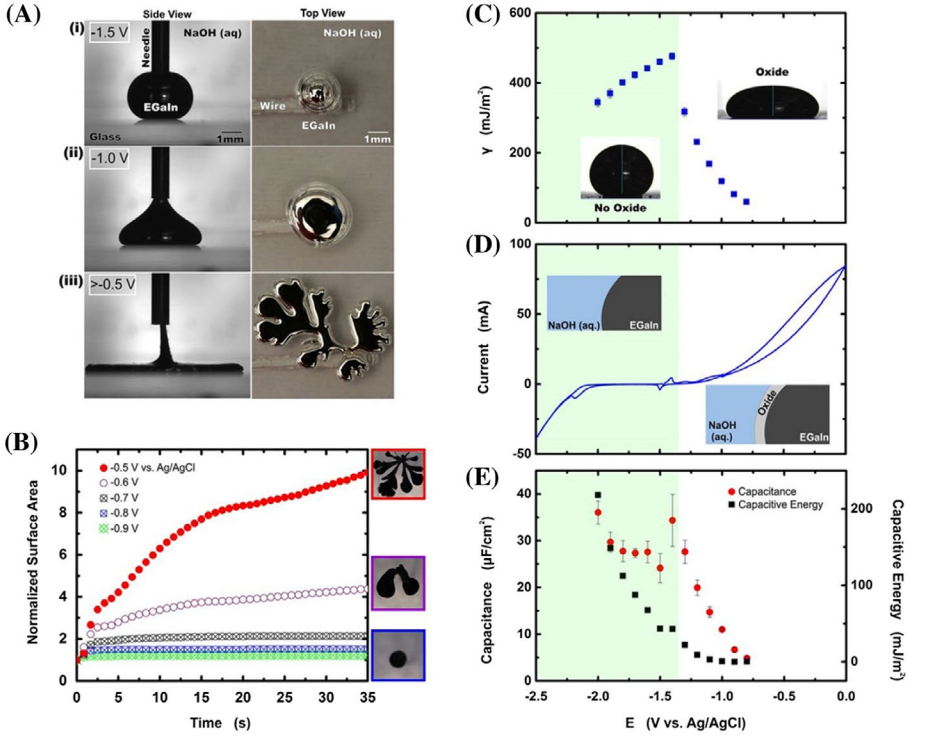

Figure 15. (a) shows images for EGaIn spread dramatically in electrolyte to response low voltage. (a i) Because of large surface tension for EGaIn droplet, it is in spherical shape. (a ii) When oxidative potential is applied, the droplet reaches a new equilibrium shape. (a iii) When the potential above critical voltage, droplet spreads and flattens and finally forms to fingering shape. (b) The areal footprint of EGaIn marble as a function of time and potential. (c) EGaIn electrocapillary curve analysed by marble shape in 1 M NaOH. (d) The cyclic voltammogram of EGaIn marble. (e) The measured capacitance and calculated capacitive energy in this range [62].

transformed quickly and reversibly. Based on these merits, a wide range of applications can be developed, such as microelectromechanical systems (MEMS) switches and conductive microcomponents [62]. Tokuda et al. demonstrated novel manipulation of liquid metal with a vision to expand the work on shape changing, programmable material and consider its use as a method for providing a programmable electric circuit [63]. Figure 16 shows work mechanism for liquid metal deformation, and the liquid metal can deform in a desired shape by adjusting the voltages among the electrode array. These techniques provide a new platform to realise novel manipulation and detailed 2D control of liquid metals under a programmable electric circuit [63].

Patterning

Ga and its alloys provide a wide range of advantages for microscale patterning. For instance, they can be injected into channels, cavities and surfaces and the wetting performance and rheological can be affected by oxide skin of Ga-based liquid metals [64]. The technology of liquid metal patterning can be separated into

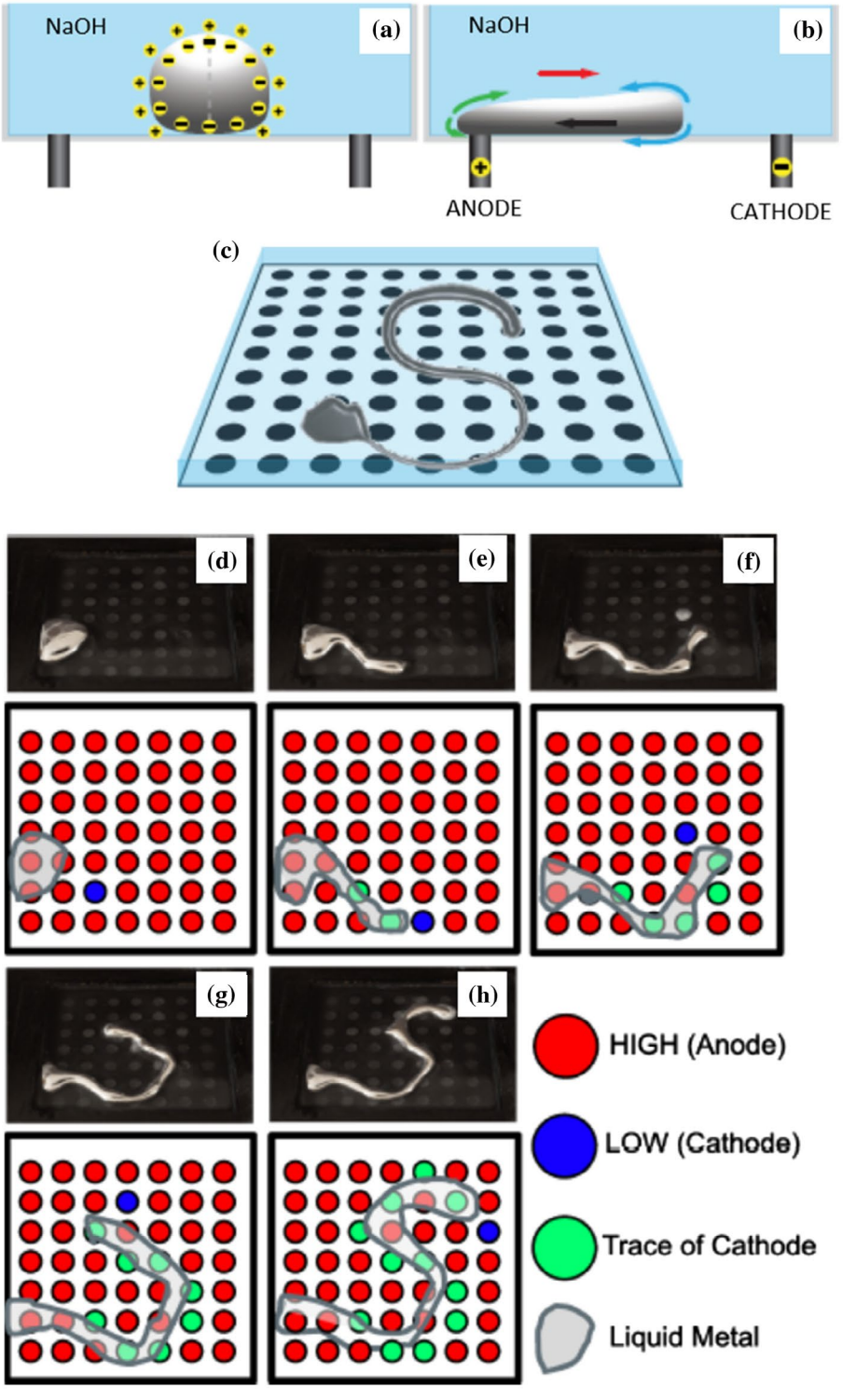

Figure 16. (a–c) shows electric potential causes deformation. (a) A liquid metal marble far from two electrodes without electric potential. (b) When the marble contact one of the electrodes and electric potential is applied. (c) Deformation of this marble as 2D process. (d–h) Basic electrode array control algorithm to make alphabet letter 'S' [63].

several categories, such as imprinting, direct patterning and addictive, the related progresses on this topic has been already reviewed [64,65]. For patterning liquid metal, imprinting metal in PDMS is an easy approach. Gozen et al. introduced the procedure for patterning liquid metal by imprinting (Figure 17(a)) [66]. Firstly, EGaIn is placed on a flat surface, then an elastomeric mould presses EGaIn and liquid metal is forced into recesses of mould. As the oxide skin forms at the surface of EGaIn, the liquid metal is wetting on PDMS, and it adhere to the cavity walls even after removing the mould from the flat surface. This method can generate two microns line width and submicron depth liquid metal traces [66]. Lu et al. reported a novel method which is utilising laser cutters for direct patterning liquid metal [67]. Figure 17(b)–(e) shows the way for direct patterning of laser, CO2 laser cutter was utilised to remove liquid metal. The liquid metal is sandwiched by two PDMS layers, the top PDMS layer can absorb the initial highly laser light and protect EGaIn to avoid excessive oxidation during laser cutting. The CO2 laser trance is applied to location, then the selected local area is removed, the liquid metal is patterned [67]. Addictive methods, especially 3D printing, can use computer-aided-design (CAD) to pattern complex and out-of-plane geometries to realise user customisation. Figure 18 shows liquid metal wires and a liquid metal droplet tower. It demonstrates this method can print 2D and three-dimensional (3D) structures [68].

High chemical reactivity and its applications

Like many post-transition metals, Ga and its alloys rapidly form an oxide skin on the surface of the metal when exposed to oxygen. The density and melting point

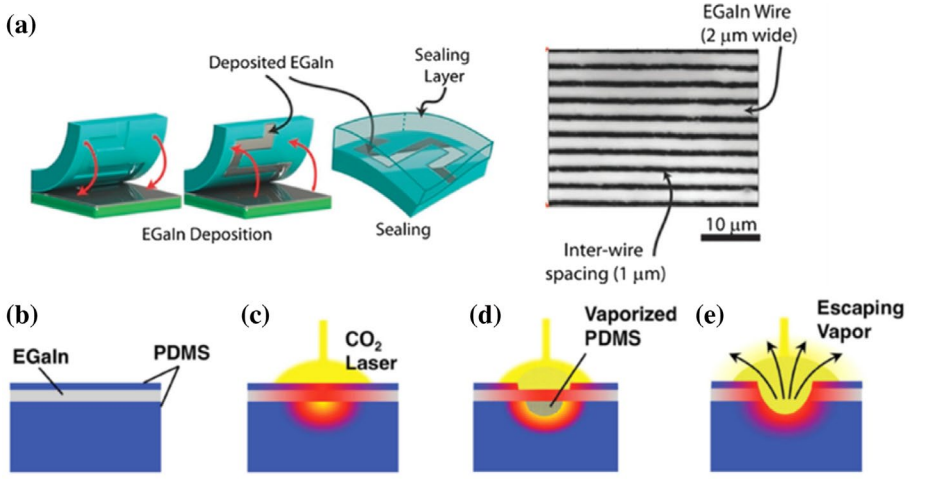

Figure 17. (a) Patterning liquid metals by imprinting [66]. (b–e) Direct patterning liquid metal by laser. (b) liquid metal is sandwiched by two PDMS layer. (c) CO_2 laser traces are applied. (d) PDMS vapourised on local area. (e) vapour escaping result in liquid metal is patterned [67].

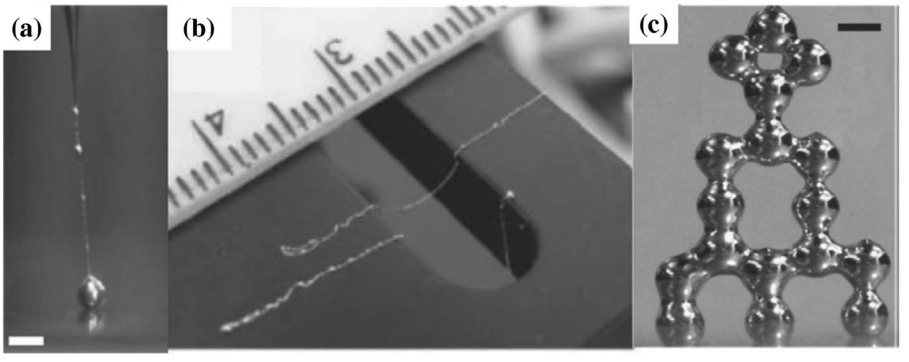

Figure 18. (a) Liquid metal wires are made by additive patterning. (b) Liquid metal wires suspend on a gap. (c) A tower of liquid metal droplets [68].

of a metal, taken together, can give a useful qualitative guide to the chemical reactivity of the metal, which means low density and low melting point indicate high reactivity [69]. For Ga-based liquid metal alloys which melting point less than room temperature, their surface show higher chemical activities owning to the diffusing metal atoms without lattice binding. Due to these specific features, Ga and its alloys provide an ideal reaction environment for the fabrication of nanomaterials [70].

Template for the growth of 2D materials

Two-dimensional (2D) materials display many outstanding features [71–74]. There are many methods to fabricate 2D materials, such as the exfoliation technique, atomic layer deposition [75] and chemical vapour deposition [76,77], but finding a method to make high-quality, large-area and large-scale 2D sheets remains a great challenge. Carey et al. introduced an approach to transform the native surface metal oxide layer of low melting point metal precursors to fabricate 2D metal chalcogenide compounds [70]. This novel method can synthesise large-area 2D semiconducting GaS through changing the oxide skin of the interfacial metal, and the metal is in the liquid state at room temperature. They selected a substrate to make the negative pattern for a photoresist (Figure 19(a)), choosing area to expose to cover vapour perflourodecyltriethoxysilane (FDTES) (Figure 19(b)). Figure 19(c) shows that liquid Ga is placed on substrate, then removed by PDMS, leaving a cracked layer of Ga oxide skin. After this process, only the Ga oxide layer is left, and the corresponding patterns are still visible. Figure 18(d) displays how hydrochloric acid (HCl) vapour treatment is utilised in intermediary processing before sulphurisation of the oxide. This is done because Ga oxide is chemically inert, and requires high temperature and toxic H_2S. The gallium oxide is transformed into $GaCl_3$, and then S vapour is used to sulphurise the $GaCl_3$ at low temperature to form GaS (Figure 19(d)). This technique can be extended to make other 2D metal materials. Because many metallic elements can be alloyed

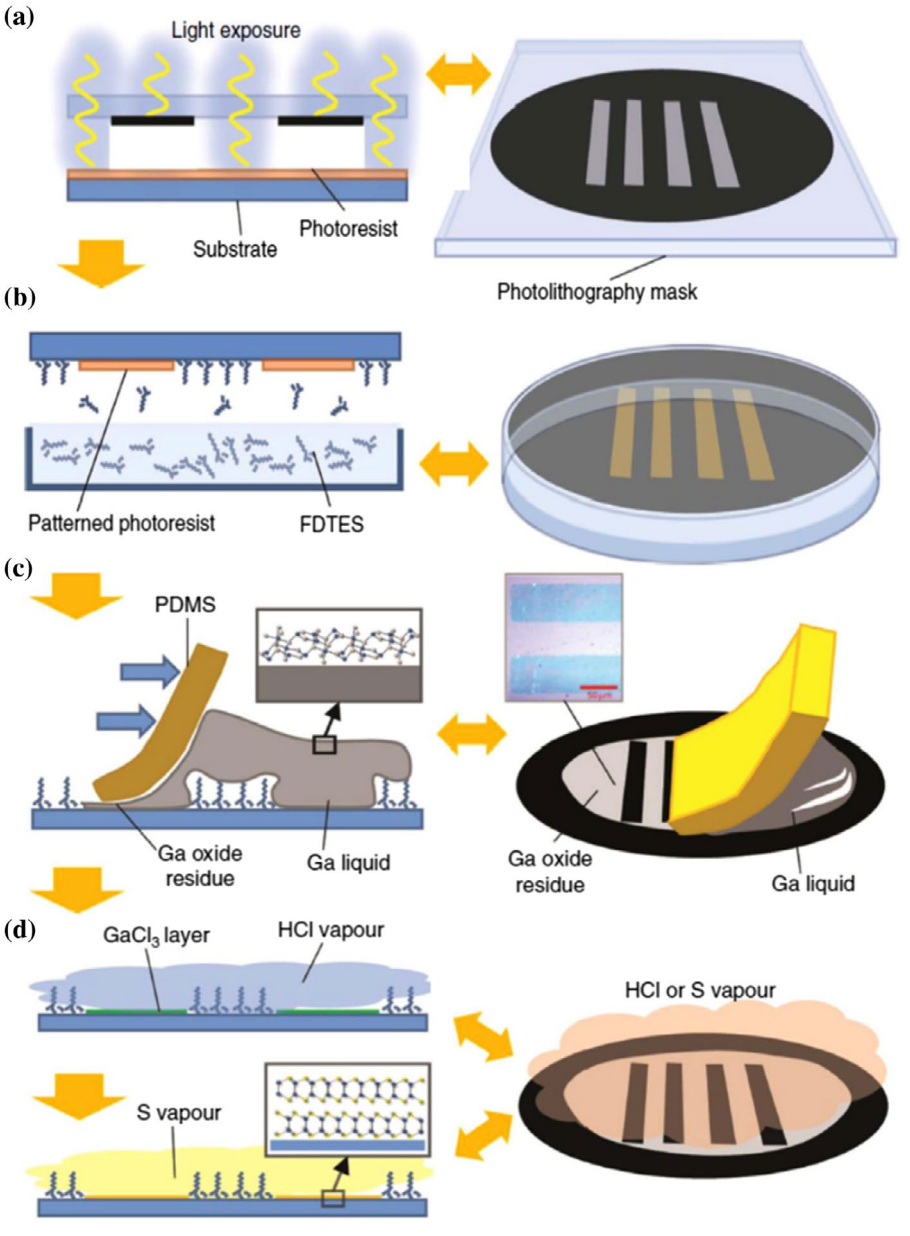

Figure 19. Schematic illustration of the printing process for GaS 2D layers. (a) Fabricating the negative pattern of the photoresist. (b) Utilising vapourised FDTES to cover the exposed surface of the substrate. (c) Placing gallium on the substrate, then removing it and leaving gallium oxide layer. (d) Firstly, HCl vapour is used to form a $GaCl_3$ layer. Then, this layer is exposed to S vapour to form GaS [70].

with gallium, this means that gallium can provide a reaction environment to make 2D metal compounds [70].

In addition to chalcogenide compounds, liquid metals can offer reaction environments to synthesis 2D oxide nanomaterials. Zavabeti et al. utilised Ga

alloys as reaction media to produce oxide nanomaterials, including HfO_2, Al_2O_3 and Gd_2O_3 [78]. As Ga and its alloys can form a self-limiting oxide skin in the metal–air interface [20,79,80], the oxide layer can be seen as a naturally formed 2D material. Based on the thermodynamic considerations, the composition of the oxide layer depends on the Gibbs free energy of the reactive metal (Figure 20(a)). The Gibbs free energy values of surface oxides are lower than that of Ga oxide. After the formation of oxide, they used the van der Waals exfoliation technique (Figure 20(b)) and the gas injection method (Figure 20(c)) to fabricate 2D nanosheets. These two steps are scalable and do not need complex systems. In this approach, liquid metal offers an environment during the reaction. This method should be suitable to fabricate oxides of many metals, and some of the oxides are significant because they have electronic, catalytic and other performance capabilities [78].

Biocompatibility and its applications

The toxicity of mercury limited its clinical application, however, unlike Hg, Ga and its alloys show a wide range of benefits, such as low toxicity and biocompatibility. Compared with conventional biomaterials, liquid metal can provide novel capabilities and solutions due to its high conductivity and liquid feature [81].

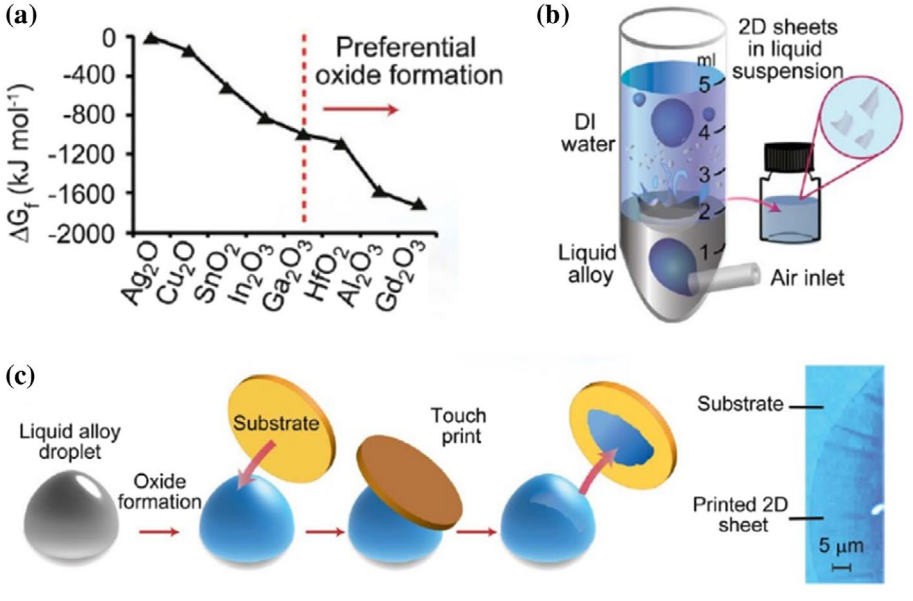

Figure 20. Fundamentals of the synthesis technique. (a) The Gibbs free energy of reactive metal oxides. (b) Schematic illustration of the van der Waals exfoliation method. (c) Schematic illustration of the gas injection approach [78].

Nerve connection

Movement disorders mainly caused by Peripheral nerve injury (PNI) are a serious problem worldwide [82–88]. Minev et al. fabricated soft neural implants with the elasticity and shape of dura mater that have displayed long-term functionality [89]. Although there are many studies on nerve function with respect to anatomy and microsurgical techniques [90], the reasons for partial or complete loss of function represent a big challenge for basic research and clinical practice [91,92]. Traditionally, nerve auto-grafting has been a common approach to repair nerves [93], but it is limited by the problems of donor grafts and matching dimensions [94]. Recently, Ga-based liquid metal has been found to provide an effective method for regeneration of peripheral nerve functional channels [95]. It is simple to fabricate, and convenient in surgical operation [96], and can be deformed *in vivo*. In addition, the electrical conductivity is much higher than in non-metallic materials. Therefore, it is a relative ideally biomaterial for PNI treatment [95]. Liu et al. proposed an approach that utilises EGaInSn for peripheral neurotmesis treatment [95]. The experiment was on bullfrogs' sciatic nerves (Figure 21(a)). An electric stimulus is applied to stimulate the nerve. After the nerve is reconnected by the liquid metal or Ringer's solution, the signal from the distal nerve was similar to that of an intact sciatic nerve (Figure 21(b) left). The difference was obvious, however, especially at the troughs and the peaks (Figure 21(b) right). EGaInSn can be combined with nerve conduits to achieve recovery of function in the period of regeneration (Figure 21(c)). EGaInSn displays many properties that

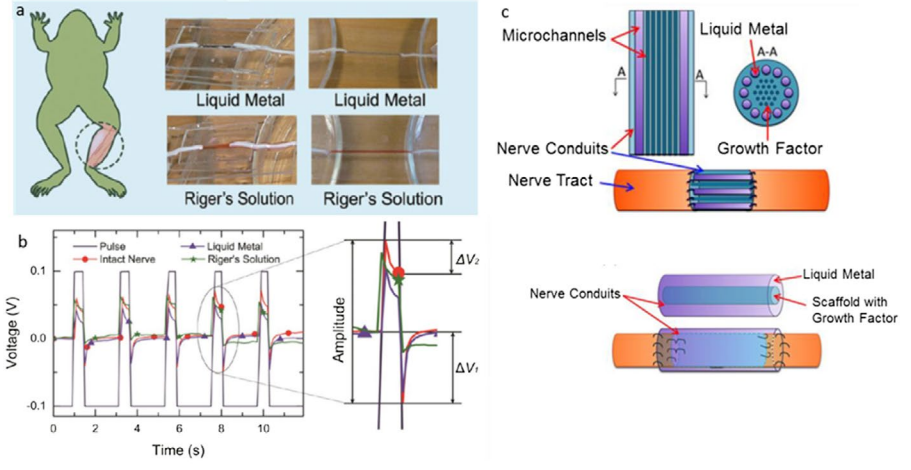

Figure 21. Schematic illustration of nerve connection by liquid metal. Images of nerve reconnected by liquid metal. (a) Schematic image of transected sciatic nerve reconnected by liquid metal and Ringer's solution, respectively. A little red ink was added into the Ringer's solution to separate it from the liquid metal. (b) The electroneurographic signal: on the left, it shows the electric-stimulus signal and the excitement signal from the intact nerve, which is connected by EGaIn or Ringer's solution. On the right, amplified details are shown of a partial view. (c) Three kinds of nerve conduits to repair the injured peripheral nerve, including a nerve conduit with microchannels and a nerve conduit with concentric tubes [95].

most conventional materials don't possesses, it is significant for future research and clinical practice, and it provides opportunities for deep research on many scientific issues [81,95].

Therapeutic use for tumours

The growth of tumour relies on the supply of blood, oxygen and nutrients [97,98]. The techniques of radiotherapy and chemotherapy are generously used in clinics along with surgical resection [81]. Nevertheless, there are many serious side effects. For instance, the tumours might be destroyed by chemotherapy and radiotherapy, but normal tissues might be damaged simultaneously, while the immune system could be destroyed. Compared with ablation, liquid metals have a huge potential to offer a gentle approach to tumour therapy [81,97]. Wang et al. proposed a method for vascular embolisation treatment. Liquid metal (EGaIn alloy) is utilised as an embolic agent to starve the target tumours to death [97]. EGaIn could be injected into vascular vessels to fill them continuously and directly. Normally, tissues are supplied with continuous nutrition and oxygen from the blood (Figure 22(a)). Although the vessel embolism could block the blood supply, the stream can be transmitted when the blockage does not occlude the blood

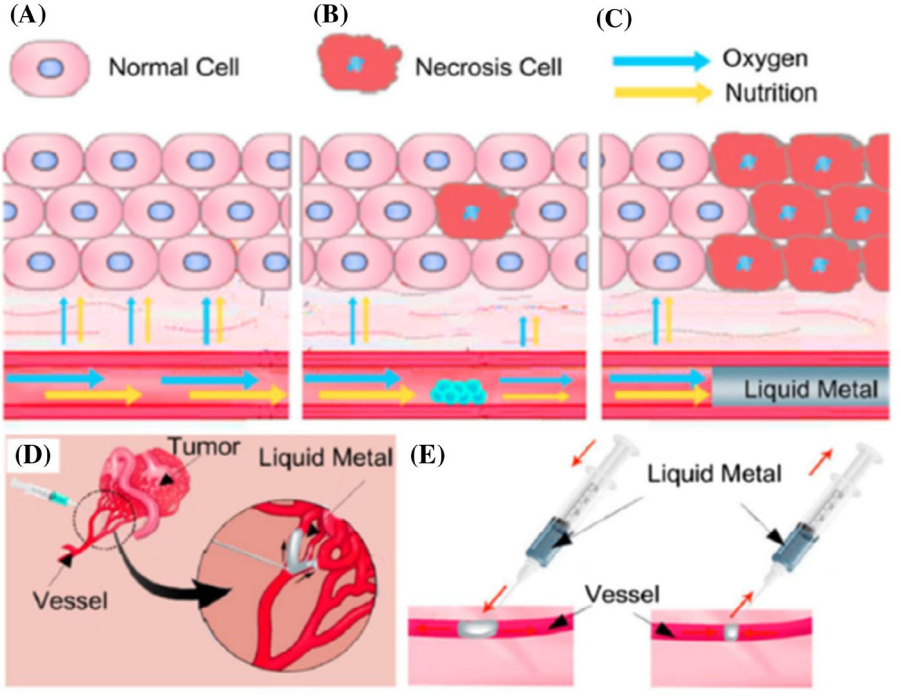

Figure 22. Schematic illustration of tumour vascular embolization therapy by liquid metal. (a) Oxygen and nutrition are supplied from vessels and tissues without embolic agents. (b) Incomplete occlusion. (c) Complete occlusion by the liquid metal. (d) The physical occlusion of the blood supply to the tumour. (e) The liquid metal could be injected into or removed from the vessel in case of need [97].

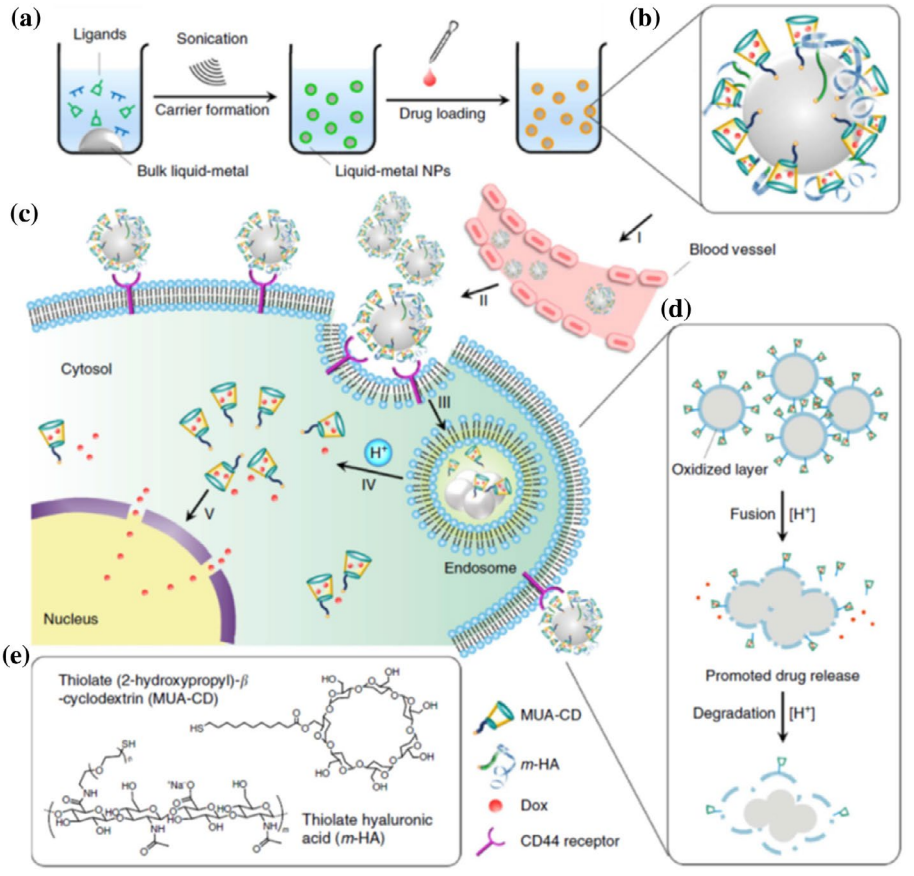

Figure 23. Schematic illiustration of liquid metal drug delivery system. (a) The route for LM-NP/Dox-L. (b) The thiolated CD with Dox, HA-based targeting motif, and an EGaIn core are main components for LM-NP/Dox-L. (c) LM-NP/Dox for the targeted tumour treatment. (I) Accumulation of LM-NP/Dox-L on the tumour sites. (II) The receptors are overexpressed by binding. (III) Receptor-mediated endocytosis; (IV) Acid-triggered fusion of LM-NP/Dox-L and endosomal/lysosomal escape of Dox-containing ligands; (V) Accumulation of Dox in the nucleus. (d) The process for fusion and degradation of LM-NP/Dox-L. (e) Chemical structures of MUA-CD and m-HA [12].

supply completely (Figure 22(b)). The EGaIn embolic agent could be shaped easily in vessels and fully occlude the micro-channels (Figure 22(c)). As the tumour relies on the oxygen and nutrients that are supplied from the blood vessels, EGaIn could causes occlusion and tumour regression (Figure 22(d)). Moreover, EGaIn can be removed after completing the therapy (Figure 22(e)). Wang et al. demonstrated that EGaIn shows low toxicity and is acceptable for clinical practice based on the evaluation of Cell Counting Kit-8 (CCK-8) and flow cytometry experiments *in vitro* In this approach, EGaIn displays flexibility and it could match the vessels perfectly [81,97]. Therefore, liquid metal is an excellent agent for tumour treatment in the future.

Drug delivery

As inorganic nanoparticles display numerous advantages in drug delivery for the treatment of diseases, several inorganic nanocarriers have been created for targeted treatment [99–103]. These approaches are limited by certain factors, however, such as toxicity and lack of biodegradability [12]. Lu et al. reported a method to use Ga-based liquid metal nanoparticles for drug delivery, owing to the low toxicity of Ga and its alloys [12,104]. They use EGaIn-based drug nanocarriers that are assembled with thiolated ligands on the surfaces of these nanoparticles through ultrasonication around room temperature. The two ligands are thiolated (2-hydroxypropyl)-b-cyclodextrin (designated as MUA-CD) and thiolated hyaluronic acid (designated as m-HA), which are not only agents protecting EGaIn nanoparticles, but also have an important part in drug loading. The final particle (designated as LM-NP/L) comprises three parts: a liquid metal (EGaIn) core, a CD-based drug-loading motif and a targeting HA ligand. The loading sites for doxorubicin (Dox, a chemotherapeutic drug) are offered by the seven-membered sugar ring of the CD [100]. Figure 23 shows the delivery system for liquid metal. Figure 23(a) and (b) show the preparation processes and components of LM-NP/Dox-L. Figure 23(c) and (d) introduces LM-NP/Dox-L for cancer therapy, and then explains the procedure of fusion and degradation. The chemical structures of MUA-CD and m-HA are shown in Figure 23(e). This novel drug delivery platform can be easily formed and assembled by ultrasonication. As a result, these nanoparticles can be fused for promoting drug release, and finally be degraded under mild acidic conditions. Furthermore, LM-NP/L has been investigated, and it shows no obvious toxicity. This system demonstrates that the liquid metal system is a good and novel platform for drug delivery [12].

Conclusion and outlook

Although liquid metal has been achieved great attention for a long time, Ga-based liquid metals are novel and significant materials that can be used for various applications in many industries due to their specific performance. In this review, we have focused on two major aspects: their physical, chemical and biological properties; then we classify these applications based on the related properties. With recent recognition of these properties, the potential to fabricate electronic components, superconductors and biomaterials has appeared. It is regarded that the Ga-based liquid metals still have much more potential to be utilised in the field of electronic fabrication, superconducting and energy biocompatibility. Many new materials integrated with liquid metal can also be envisioned and extended in different filed.

Disclosure statement

No potential conflict of interest was reported by the authors.

Funding

This work was financially supported by Australian Research Council (ARC) Discovery Projects [DP140102581], [DP160102627], [DP170101467].

ORCID

Yi Du http://orcid.org/0000-0003-1932-6732

References

[1] C.B. Eaker and M.D. Dickey, Appl. Phys. Rev. 3 (2016) p.031103.
[2] M.D. Dickey and A.C.S. Appl, Mater. Interfaces 6 (2014) p.18369.
[3] C. Buzea and K. Robbie, Supercond. Sci. Technol. 18 (2004) p.R1.
[4] K.A. Narh, V.P. Dwivedi, J.M. Grow, A. Stana and W.Y. Shih, J. Mater. Sci. 33 (1998) p.329.
[5] *Gallium-Indium Binary Alloy Phase Diagram* (based on 1969 Predel B.)
[6] D.S. Evans and A. Prince, Metal Sci. 12 (1978) p.411.
[7] K.E. Spells, Proc. Phys. Soc. London 48 (1936) p.299.
[8] M.D. Dickey, Adv. Mater. 29 (2017) p.1606425.
[9] F. Barbier and J. Blanc, J. Mater. Res. 14 (1999) p.737.
[10] E. Palleau, S. Reece, S.C. Desai, M.E. Smith and M.D. Dickey, Adv. Mater. 25 (2013) p.1589.
[11] K. Khoshmanesh, S.Y. Tang, J.Y. Zhu, S. Schaefer, A. Mitchell, K. Kalantar-zadeh and M.D. Dickey, Lab Chip 17 (2017) p.974.
[12] Y. Lu, Q. Hu, Y. Lin, D.B. Pacardo, C. Wang, W. Sun, F.S. Ligler, M.D. Dickey and Z. Gu, Nat. Commun. 6 (2015) p.889.
[13] T. Liu, P. Sen and C.J. Kim, J. Microelectromech. Syst. 21 (2012) p.443.
[14] M.J. Regan, H. Tostmann, P.S. Pershan, O.M. Magnussen, E. Dimasi, B.M. Ocko and M. Deutsch, Phys. Rev. B 55 (1997) p.786.
[15] C.B. Eaker and M.D. Dickey, Proc. SPIE 9467, Micro- Nanotech. Sens. Syst. Appl. VII (2015) p.946708.
[16] N. Kazem, T. Hellebrekers and C. Majidi, Adv. Mater. 29 (2017) p.1605985.
[17] D. Morales, N.A. Stoute, Z. Yu, D.E. Aspnes and M.D. Dickey, Appl. Phys. Lett. 109 (2016) p.091905.
[18] N.F. Mott, Proc. R. Soc. London, Ser. A. 146 (1934) p.465.
[19] C. Dodd, Proc. Phys. Soc. Section B 63 (1950) p.662.
[20] M.D. Dickey, R.C. Chiechi, R.J. Larsen, E.A. Weiss, D.A. Weitz and G.M. Whitesides, Adv. Funct. Mater. 18 (2008) p.1097.
[21] J.H. So, J. Thelen, A. Qusba, G.J. Hayes, G. Lazzi and M.D. Dickey, Adv. Funct. Mater. 19 (2009) p.3632.
[22] L. Ren, J. Zhuang, G. Casillas, H. Feng, Y. Liu, X. Xu, Y. Liu, J. Chen, Y. Du, L. Jiang and S.X. Dou, Adv. Funct. Mater. 26 (2016) p.8111.
[23] K.Q. Ma and J. Liu, J. Phys. D: Appl. Phys. 40 (2007) p.4722.
[24] Y. Deng and J. Liu, Heat Mass Transf. 46 (2010) p.1327.
[25] T. Li, Y.G. Lv, J. Liu and Y.X. Zhou, Forsch. Ingenieurwes 70 (2005) p.243.
[26] J.Y. Zhu, S.Y. Tang, K. Khoshmanesh and K. Ghorbani, ACS Appl. Mater. Interfaces 8 (2016) p.2173.
[27] W. Shen, R.T. Edwards and C.J. Kim, J. Microelectromech Syst. 15 (2006) p.879.
[28] P.A. Giguère and D. Lamontagne, Science 120 (1954) p.390.
[29] P. Surmann and H. Zeyat, Anal. Bioanal. Chem. 383 (2005) p.1009.

[30] S. Zhu, J.H. So, R. Mays, S. Desai, W.R. Barnes, B. Pourdeyhimi and M.D. Dickey, Adv. Funct. Mater. 23 (2013) p.2308.
[31] G.J. Hayes, J.H. So, A. Qusba, M.D. Dickey, G. Lazzi and I.E.E.E. Trans, Antennas Propag. 60 (2012) p.2151.
[32] M.G. Mohammed and M.D. Dickey, Sens. Actuators A: Phys. 193 (2013) p.246.
[33] K. Ling, K. Kim and S. Lim, Opt. Express 23 (2015) p.21375.
[34] D.H. Kim, J.H. Ahn, W.M. Choi, H.S. Kim, T.H. Kim, J. Song, Y.Y. Huang, Z. Liu, C. Lu and J.A. Rogers, Science 320 (2008) p.507.
[35] D. Kim, J. Xiao, J. Song, Y. Huang and J.A. Rogers, Adv. Mater. 22 (2010) p.2108.
[36] M.C. LeMieux and Z. Bao, Nat. Nanotechnol. 3 (2008) p.585.
[37] J.A. Rogers, T. Someya and Y. Huang, Science 327 (2010) p.1603.
[38] M.R. Khan, G.J. Hayes, S. Zhang, M.D. Dickey and G. Lazzi, I.E.E.E. Microw. Wirel 22(11) (2012) p.577.
[39] A. Taslimi and K. Mouthaan, Proc. IEEE Int. Conf. Wireless Inform. Technol. Syst. (ICWITS) (2010) p.1.
[40] J.T. Bernhard, Synth. Lectures Antennas 2 (2007) p.1.
[41] M. Wang, M.R. Khan, C. Trlica, M.D. Dickey and J.J. Adams, Proc. IEEE Int. Symp. Antennas Propag. (2015) p. 2223.
[42] K.A. Williams, A.J. Boydston, C.W. and Bielawski, J. R. Soc. Interface 4 (2007) p.359.
[43] G. Li, X. Wu and D.W. Lee, Lab Chip 16 (2016) p.1366.
[44] M. Carano and J. Fjelstad, *Electronic Materials and Processes Handbook*, 3rd ed., McGraw-Hill, New York, NY, 2004, ch. 7, p. 1.
[45] R. Lerdwanittip, A. Namsang and P. Akkaraekthalin, J. Semicond. Technol. Sci. 11(1) (2011) p.65.
[46] B.L. Cumby, G.J. Hayes, M.D. Dickey, R.S. Justice, C.E. Tabor and J.C. Heikenfeld, Appl. Phys. Lett. 101(17) (2012) p.174102.
[47] A. Dey, R. Guldiken and G. Mumcu, Proc. IEEE Antennas Propag. Soc. Int. Symp. (APS-URSI) (2013) p. 392.
[48] M. Rashed Khan, G.J. Hayes, J.H. So, G. Lazzi and M.D. Dickey, Appl. Phys. Lett. 99 (2011) p.013501.
[49] M.D. Dickey, R.C. Chiechi, R.J. Larsen, E.A. Weiss, D.A. Weitz and G.M. Whitesides, Adv. Funct. Mater. 18 (2008) p.1097.
[50] S.Y. Tang, Y. Lin, I.D. Joshipura, K. Khoshmanesh and M.D. Dickey, Lab Chip 15 (2015) p.3905.
[51] T. Liu, P. Sen and C.J. Kim, IEEE 23rd Int. Conf. Micro Electro Mech. Syst. (MEMS) (2010) p. 560.
[52] C. Quilliet and B. Berge, Curr. Opin. Colloid Interface Sci. 6 (2001) p.34.
[53] D. Avnir, J. Chem. Educ. 66 (1989) p.211.
[54] R.C. Gough, J.H. Dang, A.M. Morishita, A.T. Ohta and W.A. Shiroma, Proc. IEEE Asia-Pacific Microw. Conf. (APMC'14) (2014) p.932.
[55] L. Hu, L. Wang, Y. Ding, S. Zhan and J. Liu, Adv. Mater. 28 (2016) p.9210.
[56] S. Holcomb, M. Brothers, A. Diebold, W. Thatcher, D. Mast, C. Tabor and J. Heikenfeld, Langmuir 32 (2016) p.12656.
[57] A. Zavabeti, T. Daeneke, A.F. Chrimes, A.P. O'Mullane, J.Z. Ou, A. Mitchell and K. Kalantar-Zadeh, Nat. Commun. 7 (2016) p.12402.
[58] S.Y. Tang, K. Khoshmanesh, V. Sivan, P. Petersen, A.P. O'Mullane, D. Abbott, A. Mitchell and K. Kalantar-zadeh, Proc. Natl. Acad. Sci. U.S.A. 111 (2014) p.3304.
[59] J.Y. Zhu, P. Thurgood, N. Nguyen, K. Ghorbani and K. Khoshmanesh, Lab Chip 17 (2017) p.3862.

[60] S.Y. Tang, V. Sivan, K. Khoshmanesh, A.P. O'Mullane, X. Tang, B. Gol and K. Kalantar-Zadeh, Nanoscale 5 (2013) p.5949.
[61] S.Y. Tang, V. Sivan, P. Petersen, W. Zhang, P.D. Morrison, K. Kalantar-zadeh, A. Mitchell and K. Khoshmanesh, Adv. Funct. Mater. 24 (2014) p.5851.
[62] M.R. Khan, C.B. Eaker, E.F. Bowden and M.D. Dickey, Proc. Natl. Acad. Sci. U.S.A. 111 (2014) p.14047.
[63] Y. Tokuda, J. L. B. Moya, G. Memoli, T. Neate, D. R. Sahoo, S. Robinson and S. Subramanian, Proc. 2017 ACM Int. Conf. Interactive Surf. Spaces (2017) p.142.
[64] I.D. Joshipura, H.R. Ayers, C. Majidi and M.D. Dickey, J. Mater. Chem. C 3 (2015) p.3834.
[65] M.A.H. Khondoker and D. Sameoto, Smart Mater. Struct. 25 (2016) p.093001.
[66] B.A. Gozen, A. Tabatabai, O.B. Ozdoganlar and C. Majidi, Adv. Mater. 26 (2014) p.5211.
[67] T. Lu, L. Finkenauer, J. Wissman and C. Majidi, Adv. Funct. Mater. 24 (2014) p.3351.
[68] C. Ladd, J.H. So, J. Muth and M.D. Dickey, Adv. Mater. 25 (2013) p.5081.
[69] M. Laing, J. Chem. Educ. 78 (2001) p.1054.
[70] B.J. Carey, J.Z. Ou, R.M. Clark, K.J. Berean, A. Zavabeti, A.S. Chesman, S.P. Russo, D.W. Lau, Z.Q. Xu, Q. Bao and O. Kevehei, Nat. Commun. 8 (2017) p.14482.
[71] M. Xu, T. Liang, M. Shi and H. Chen, Chem. Rev. 113 (2013) p.3766.
[72] K.S. Novoselov, A.K. Geim, S. Morozov, D. Jiang, M. Katsnelson, I. Grigorieva, S. Dubonos and A.A. Firsov, Nature 438 (2005) p.197.
[73] Q.H. Wang, K. Kalantar-Zadeh, A. Kis, J.N. Coleman and M.S. Strano, Nat. Nanotechnol. 7 (2012) p.699.
[74] P. Miro, M. Audiffred and T. Heine, Chem. Soc. Rev. 43 (2014) p.6537.
[75] L.K. Tan, B. Liu, J.H. Teng, S. Guo, H.Y. Low and K.P. Loh, Nanoscale 6 (2014) p.10584.
[76] S. Balendhran, J.Z. Ou, M. Bhaskaran, S. Sriram, S. Ippolito, Z. Vasic, E. Kats, S. Bhargava, S. Zhuiykov and K. Kalantar-zadeh, Nanoscale 4 (2012) p.461.
[77] Z.Q. Xu, Y. Zhang, S. Lin, C. Zheng, Y.L. Zhong, X. Xia, Z. Li, P.J. Sophia, M.S. Fuhrer, Y.B. Cheng and Q. Bao, ACS Nano 9 (2015) p.6178.
[78] A. Zavabeti, J.Z. Ou, B.J. Carey, N. Syed, R. Orrell-Trigg, E.L. Mayes, C. Xu, O. Kavehei, A.P. O'Mullane, R.B. Kaner and K. Kalantar-zadeh, Science 358 (2017) p.332.
[79] N. Cabrera and N.F. Mott, Rep. Prog. Phys. 12 (1949) p.163.
[80] D. Kim, P. Thissen, G. Viner, D.W. Lee, W. Choi, Y.J. Chabal, J.B. Lee and A.C.S. Appl, Mater. Interfaces 5 (2012) p.179.
[81] L. Yi and J. Liu, Int. Mater. Rev. 62 (2017) p.1.
[82] S.K. Lee and S.W. Wolfe, J. Am. Acad. Orthop. Surg. 8 (2000) p.243.
[83] A.D. Widgerow, A.A. Salibian, E. Kohan, T. Sartiniferreira, H. Afzel, T. Tham and G.R. Evans, Microsurgery 34 (2014) p.324.
[84] J. Scheib and A. Höke, Nat. Rev. Neurol. 9 (2013) p.668.
[85] J. Kimura, *Electrodiagnosis in diseases of nerve and muscle: principles and practice*, Oxford University Press, Oxford, 2001, p.140.
[86] K.L. McCance and S.E. Huether, *Pathophysiology: the biologic basis for disease in adults and children*, Elsevier Health Sciences, Amsterdam, 2014, p. 79.
[87] D.A. McCormick and J.R. Huguenard, J. Neurophysiol. 68 (1992) p.1384.
[88] M. Hubli and V. Dietz, J. Neuroeng. Rehabil. 10 (2013) p.5.
[89] I.R. Minev, P. Musienko, A. Hirsch, Q. Barraud, N. Wenger, E.M. Moraud, J. Gandar, M. Capogrosso, T. Milekovic, L. Asboth and R.F. Torres, Science 347 (2015) p.159.
[90] J. Scheib and A. Höke, Nat. Rev. Neurol. 9 (2013) p.668.
[91] S.H. Oh, J.H. Kim, K.S. Song, B.H. Jeon, J.H. Yoon, T.B. Seo, U. Namgung, I.W. Lee and J.H. Lee, Biomaterials 29 (2008) p.1601.
[92] J. Scheib and A. Höke Nat, Rev. Neurol. 9 (2013) p.668.
[93] G.R. Evans, Anat. Rec. 263 (2001) p.396.

[94] T. Gordon, O. Sulaiman and J.G. Boyd, J. Peripher. Nerv. Syst. 8 (2003) p.236.
[95] J. Zhang, L. Sheng, C. Jin and J. Liu, arXiv preprint (2014) *arXiv: 1404.5931*.
[96] C. Jin, J. Zhang, X. Li, X. Yang, J. Li and J. Liu, Sci. Rep. 3 (2013) p.3442.
[97] Q. Wang, Y. Yu and J. Liu, arXiv preprint (2014) *arXiv: 1408.0989*.
[98] E. Witsch, M. Sela and Y. Yarden, Physiology 25 (2010) p.85.
[99] D. Peer, J.M. Karp, S. Hong, O.C. Farokhzad, R. Margalit and R. Langer, Nat. Nanotechnol. 2 (2007) p.751.
[100] E.K. Chow, X.Q. Zhang, M. Chen, R. Lam, E. Robinson, H. Huang, D. Schaffer, E. Osawa, A. Goga and D. Ho, Sci. Transl. Med. 3 (2011) p.73ra21.
[101] B.P. Timko, M. Arruebo, S.A. Shankarappa, J.B. McAlvin, O.S. Okonkwo, B. Mizrahi, C.F. Stefanescu, L. Gomez, J. Zhu, A. Zhu and J. Santamaria, Proc. Natl Acad. Sci. U.S.A. 111 (2014) p.1349.
[102] C. Xu, B. Wang and S. Sun, J. Am. Chem. Soc. 131 (2009) p.4216.
[103] H.J. Kim, H. Takemoto, Y. Yi, M. Zheng, Y. Maeda, H. Chaya, K. Hayashi, P. Mi, F. Pittella, R.J. Christie and K. Toh, ACS Nano 8 (2014) p.8979.
[104] M.E. Davis and M.E. Brewster, Nat. Rev. Drug Discov. 3 (2004) p.1023.